J Therm Anal Calorim (2009) 97:507–513
DOI 10.1007/s10973-009-0369-9

Non-isothermal crystallization kinetics of some basaltic glass-ceramics containing CaF_2 as nucleation agent

C. Păcurariu · R. I. Lazău · I. Lazău · R. Ianoş · B. Tiţa

ICTAC2008 Conference

Abstract The crystallization mechanism of the glass-ceramics obtained from Romanian (Şanoviţa) basalt in the presence of 3 and 5% CaF_2 as nucleation agent has been investigated under non-isothermal conditions using DTA technique. The activation energies of the crystallization processes were calculated using the Kissinger-Akahira-Sunose, Ozawa-Flynn-Wall, Starink and Tang isoconversional methods. The monotonous decreases in the activation energy (E_a) with the crystallized fraction (α) confirms the complex mechanism of the glass-ceramics crystallization process. It has been proved that the Johnson-Mehl-Avrami model cannot be applied for the studied glass-ceramics crystallization process.

Keywords Crystallization kinetics · Glass-ceramics · Nucleation agents

Introduction

Basaltic rocks represent cheap raw materials for the glass-ceramics production. High mechanical and abrasion resistance, good chemical stability, special electrical properties or wear-resistance recommend the glass-ceramics to be used in different industrial fields like: wear resistant balls fort paints and lacquers homogenization, tiles for paving in the chemical industry, replacement for the enamels used in the industrial environments at high temperatures or glazed tiles. Also, the glass-ceramics were used as matrices for nuclear waste inertization and recently, for the vitrification of various hazardous industrial wastes [1–6].

In Romania, the basalt of Şanoviţa (Timiş) was used for obtaining some glass-ceramics, ceramic glazes and sintered products [2, 7].

The main crystalline phase in the glass-ceramic based on basalt is represented by the pyroxene solid solution $Ca(Mg, Fe)SiO_3$ [1, 2, 7–10].

The favorable effect of the nucleation agents upon the crystallization processes and the physical-mechanical properties of the resulted glass-ceramics is mentioned in the literature data [1, 2, 6, 7, 10, 11]. CaF_2, TiO_2 and ZrO_2 are amongst the most efficient nucleation agents in this field.

The present study focuses on analyzing the crystallization mechanism of the glass-ceramics obtained from the modified Şanoviţa basalt in the presence of 3 and 5% CaF_2 as nucleation agent. For the kinetic studies, a series of differential thermal analysis (DTA) under non-isothermal conditions were carried out at various heating rates.

The crystalline phases formed were identified by X-ray diffraction method.

Experimental

Samples preparation

The glass-ceramic was obtained by adjusting the oxide composition of the natural Şanoviţa basalt (Romania) [10] by the $MgCO_3$ and $CaCO_3$ addition. The oxide composition of the obtained glass-ceramic was: SiO_2, 46.39%; Al_2O_3, 10.98%; Fe_2O_3, 8.45%; CaO, 21.0%; MgO, 11.42%;

C. Păcurariu (✉) · R. I. Lazău · I. Lazău · R. Ianoş
Faculty of Industrial Chemistry and Environmental Engineering, "Politehnica" University of Timişoara, P-ţa Victoriei No. 2, 300006 Timisoara, Romania
e-mail: cornelia.pacurariu@chim.upt.ro

B. Tiţa
Faculty of Pharmacy, University of Medicine and Pharmacy "Victor Babeş", P-ţa E. Murgu no. 2, Timisoara, Romania

Na_2O+K_2O, 1.65%; TiO_2, 0.11%. To this glass-ceramic composition, 3% CaF_2 (sample BD-F3) and respectively 5% CaF_2 (sample BD-F5) was added, as nucleation agent. The synthesis method of the glass-ceramics was presented in a previous paper [11] and it is mainly based on melting the raw materials mixture followed by a fast cooling in order to obtain glass. Afterwards, the glass-ceramic material was obtained by subjecting the glass to a thermal treatment.

Characterization methods

The samples were subjected to differential thermal analysis (DTA) using a C MOM Hungary derivatograph. The DTA curves were recorded in static air atmosphere in the temperature range 25–1,000 °C at various heating rates: 4, 8, 12, 16, 20 °C min^{-1}. The sample mass was 800 mg and the reference material used was aluminum oxide.

The evolution of the samples phase composition after the thermal treatments has been assessed by XRD (Bruker's D8 Advanced system) using Ni filtered CuK_α radiation.

Kinetic analysis

The general equation of the reaction rate for non-isothermal conditions at constant heating rate is generally written as [12–16]

$$g(\alpha) = \frac{AE}{R\beta}p(x) \tag{1}$$

where $g(\alpha)$ is the conversion integral, A the pre-exponential factor, E the activation energy, R the general gas constant, β the heating rate and $p(x)$ is the temperature integral, where $x = E/RT$ is the reduced activation energy at the temperature T.

Applying different approximations for the temperature integral, a wide range of different isoconversional methods can be derived [14–22]. The general equation resulted is:

$$\ln\frac{\beta}{T_\alpha^\kappa} = -A\frac{E_\alpha}{RT_\alpha} + C \tag{2}$$

where: κ is a constant depending on the approximation of the temperature integral employed, A and C are constants and the subscript α designates values related to a given conversion degree.

In order to achieve the kinetic parameters, all of these isoconversional methods involve the plotting of the left side of Eq. 2 versus $1/T_\alpha$. In the present work, four isoconversional methods were used.

Kissinger-Akahira-Sunose method

The Kissinger-Akahira-Sunose (KAS) method, sometimes called the generalized Kissinger method is one of the best isoconversional methods. Using the Murray and White approximation [14, 15, 17, 23] for the temperature integral $p(x) \cong e^{-x}/x^2$ $(20 < x < 50)$, the KAS method is derived. At constant conversion α, this assumption leads to Eq. 3:

$$\ln\frac{\beta}{T_\alpha^2} = -\frac{E_\alpha}{RT_\alpha} + C \tag{3}$$

The more precise approximation of Coats and Redfern [14, 24]: $p(x) \cong \frac{e^{-x}}{x^2}(1 - 2/x)$, leads to the same Eq. 3.

Ozawa-Flynn-Wall method

The approximation suggested by Doyle [14, 15, 17, 25] for the temperature integral $p(x) \cong e^{-1.052x\ -\ 5.330}$, derived to the Ozawa-Flynn-Wall (OFW) method. At constant conversion α, the linear equation (4) of Ozawa-Flynn-Wall results:

$$\ln\beta = -1.052\frac{E_\alpha}{RT_\alpha} + C \tag{4}$$

Starink method

The approximation suggested by Starink [13, 14, 17] for the temperature integral is: $p(x) \cong e^{\frac{-1.0008x-0.312}{x^{1.92}}}$. At constant conversion α, this assumption leads to the Starink Eq. 5:

$$\ln\frac{\beta}{T_\alpha^{1.92}} = -1.0008\frac{E_\alpha}{RT_\alpha} + C \tag{5}$$

Tang method

The approximation proposed by Tang [26, 27] for the temperature integral is: $-\ln p(x) = 0.37773896 + 1.894661 \ln x + 1.00145033x$. At constant conversion α, this assumption leads to the Tang Eq. 6:

$$\ln\frac{\beta}{T_\alpha^{1.894661}} = -1.00145033\frac{E_\alpha}{RT_\alpha} + C \tag{6}$$

Differential thermal analysis (DTA) is very suitable for the kinetic study of the glass-ceramic crystallization under non-isothermal conditions.

The crystallized fraction was determined from the DTA curves using Eq. 7:

$$\alpha(T) = \frac{A_{(T)}}{A_{(\mathrm{Total})}} \tag{7}$$

where $\alpha(T)$ is the crystallized fraction at the temperature T, $A_{(T)}$ the area at the temperature interval ΔT and $A_{(\mathrm{Total})}$ the total area of the crystallization peak.

In order to verify the applicability of the Johnson-Mehl-Avrami (JMA) model for the non-isothermal crystallization processes of the studied glass-ceramics, the Avrami exponent n was calculated using the Ozawa method [18, 19].

Ozawa method

Ozawa proposed an extension of the Avrami [28, 29] equation (8) to describe the kinetics of non-isothermal crystallization

$$\alpha = 1 - \exp(-Kt^n) \quad (8)$$

where K and n are constants with respect to time.

At a given temperature, the equation proposed by Ozawa [19] is expressed as:

$$\log[-\ln(1-\alpha)] = \log \chi(T) - n \log \beta \quad (9)$$

where $\chi(T)$ is a constant.

The Avrami exponent n results from the slope of the plot of $\log[-\ln(1-\alpha)]$ as a function of $\log \beta$ at a given temperature.

Results and discussion

The DTA crystallization curves for the glass-ceramic with 3% CaF_2 as nucleation agent (sample BD-F3) for five different heating rates are presented in Fig. 1.

The temperatures at the maximum crystallization rate (temperatures of DTA peaks) of the BD-F5 sample for different heating rates are presented in Table 1.

The crystallized fraction α was determined from the DTA curves using Eq. 7. The dependences of the crystallized fraction on temperature for sample BD-F5 is presented for different heating rates in Fig. 2.

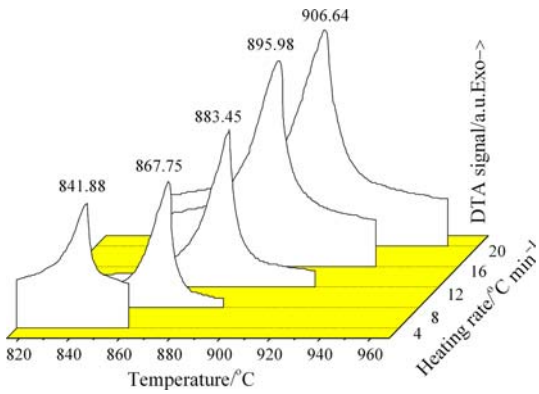

Fig. 1 DTA crystallization curves of BD-F3 sample for different heating rates

Table 1 Temperatures of DTA peaks for different heating rates of the BD sample

Heating rate/°C min^{-1}	4	8	12	16	20
Temperatures of DTA peaks/°C	825.87	849.93	867.43	878.40	889.87

Kissinger-Akahira-Sunose method

The activation energies for the crystallization processes were calculated from the slope of the linear fitted function of $\ln(\beta/T_\alpha^2)$ versus T_α^{-1} (Eq. 3), for several crystallized fractions. The KAS plots are shown in Fig. 3 for sample BD-F3.

Ozawa-Flynn-Wall method

The activation energies of the crystallization processes were also estimated by using the OFW method. For constant crystallized fraction, the value of E_a was calculated from the slope of the linear fitted function of $\ln \beta$ versus T_α^{-1} (Eq. 4). The OFW plots are presented in Fig. 4 for sample BD-F5.

Figure 5 presents comparatively, the variation of E_a, calculated with the KAS and OFW methods, with the crystallized fraction α, for the samples BD-F3 and BD-F5.

As it results from Fig. 5, the activation energies values calculated using the KAS and OFW methods, monotonously decrease with the crystallized fraction for both samples.

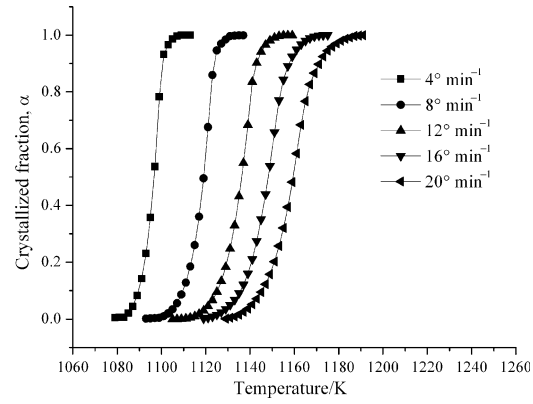

Fig. 2 Crystallized fraction α versus temperature for sample BD-F5 at different heating rate

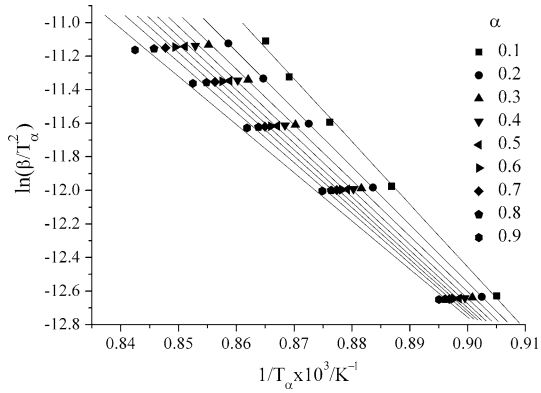

Fig. 3 Plots of $\ln(\beta/T_\alpha^2)$ versus T_α^{-1} for sample BD-F3 at different crystallized fractions

For both samples, BD-F3 and BD-F5, it can be observed the slightly smaller E_a values obtained with KAS method than those calculated with OFW method.

Starink method

Using the Starink method, the value of E_a was calculated from the slope of the linear fitted function of $\ln(\beta/T_\alpha^{1.92})$ versus T_α^{-1} (Eq. 5) for constant crystallized fraction. The Starink plots for different crystallized fractions are presented in Fig. 6 for the sample BD-F3.

Tang method

The activation energies for the crystallization processes were calculated from the slope of the linear fitted function of $\ln(\beta/T_\alpha^{1.894661})$ versus T_α^{-1} (Eq. 6), for several crystallized fractions. The Tang plots for different crystallized fractions are presented in Fig. 7 for the sample BD-F5.

The values of the activation energies for the samples BD-F3 and BD-F5, calculated with the Starink and Tang method for several crystallized fractions are presented in Table 2.

As it results from Table 2, the activation energies values calculated using the Starink and Tang methods, are very close and also, monotonously decrease with the crystallized fraction for both samples.

Correlating the activation energies values obtained with the four presented isoconversional methods, it may be noticed:

– The increase of the nucleation agent content from 3% CaF_2 in the sample BD-F3 to 5% CaF_2 in the sample BD-F5 results in a decrease of the E_a values, no matter which isoconversional method was used. These values are in accordance with our previous results and confirm the benefic role of the nucleation agent content growth on the crystallization process [11, 30].

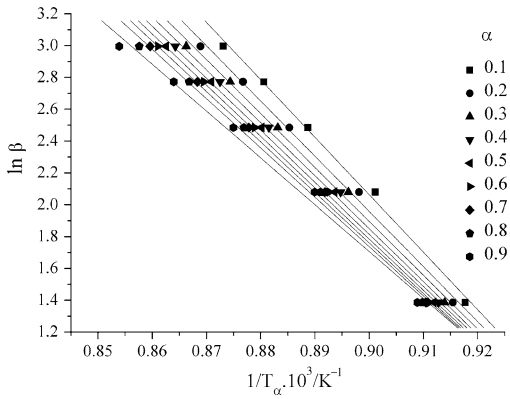

Fig. 4 Plots of ln β versus T_α^{-1} for sample BD-F5 at different crystallized fractions

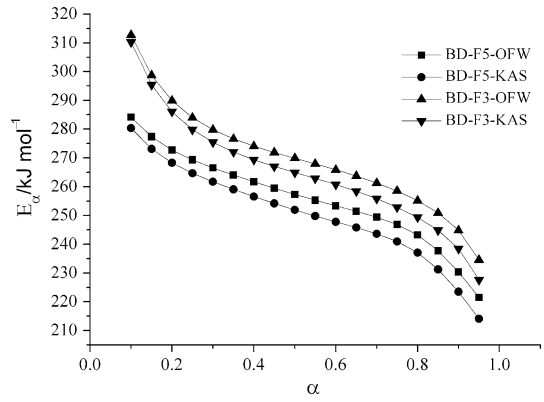

Fig. 5 Variation of E_a, calculated with the KAS and OFW methods, with α for samples BD-F3 and BD-F5

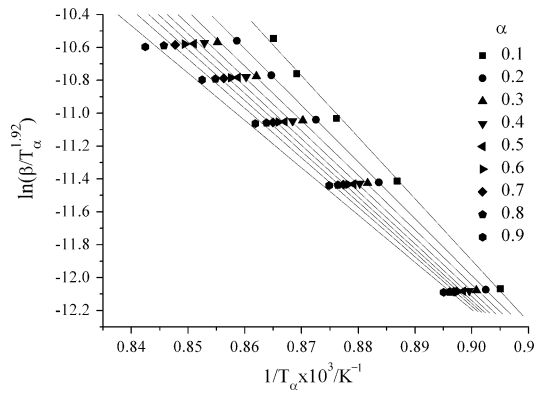

Fig. 6 Plots of $\ln(\beta/T_\alpha^{1.92})$ versus T_α^{-1} for the sample BD-F3 at different crystallized fractions

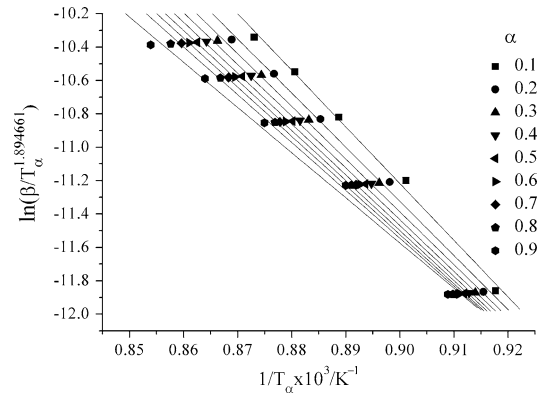

Fig. 7 Plots of $\ln(\beta/T_\alpha^{1.894661})$ versus T_α^{-1} for the sample BD-F5 at different crystallized fractions

– For both samples, the activation energies calculated with KAS, Starink and Tang equations are very close and a little smaller than the values obtained with the OFW method.
– The activation energy values decrease monotonously with the crystallized fraction for both samples no matter which isoconversional method was used. This behavior

Table 2 The activation energies and the correlation coefficients for the samples BD-F3 and BD-F5, calculated with the Starink and Tang method

α	BD-F3				BD-F5			
	Starink method		Tang method		Starink method		Tang method	
	E_a/kJ mol^{-1}	r^2	E_a/kJ mol^{-1}	r^2	E_a/kJ mol^{-1}	r^2	E_a/kJ mol^{-1}	r^2
0.1	310.71	0.9989	310.75	0.9989	280.89	0.9977	281.68	0.9977
0.2	286.63	1	286.68	1	268.83	0.9977	269.21	0.9977
0.3	275.96	0.9999	276.02	0.9999	262.25	0.9977	262.52	0.9977
0.4	269.91	0.9997	269.98	0.9998	257.13	0.9976	257.37	0.9976
0.5	265.49	0.9994	265.56	0.9997	252.46	0.9974	252.69	0.9974
0.6	261.26	0.9991	261.33	0.9991	248.33	0.9973	248.55	0.9973
0.7	256.37	0.9987	256.44	0.9987	244.18	0.9971	244.41	0.9971
0.8	249.89	0.9987	249.97	0.9982	237.61	0.9962	237.96	0.9962
0.9	239.01	0.9972	239.09	0.9973	224.03	0.9943	224.69	0.9944

is similar with the glass-ceramics crystallization in the presence of TiO_2 as nucleation agent [30, 31] and confirms the complex mechanism of the glass-ceramics crystallization process, involving probably a self-accelerating effect. As result, the calculated activation energies are apparent values, depending on the activation energies of the elementary processes (nucleation and growth) involved in the crystallization process.

In order to confirm the complex mechanism of the crystallization process and the validity of the JMA model for the studied glass-ceramics, the Avrami exponent n was determined using Ozawa method (Eq. 9). The plots of $\log[-\ln(1-\alpha)]$ versus $\log\beta$ at different temperatures for sample BD-F5 are presented in Fig. 8.

Table 3 summarizes the values of Avrami exponent calculated by using Ozawa method, for sample BD-F3 and BD-F5 at different temperatures.

As can be seen from the data in Table 3, for both samples, the Avrami exponent has values higher than four ($n > 4.0$). For BD-F5 sample (with 5% CaF_2) the Avrami exponent values are higher than for the BD-F3 sample (with 3% CaF_2). These high values for n indicate that the studied glass-ceramics crystallization cannot be described by the Johnson-Mehl-Avrami (JMA) model.

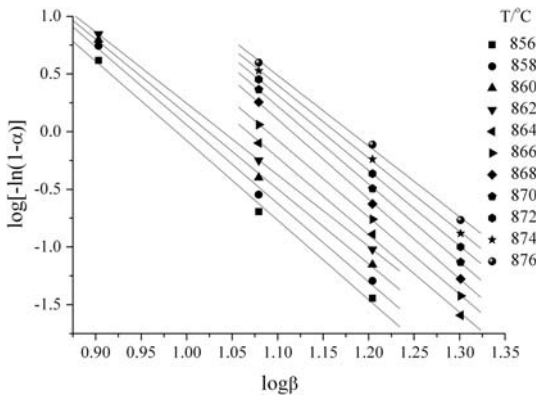

Fig. 8 Plots of $\log[-\ln(1-\alpha)]$ as a function of $\log\beta$ for sample BD-F5 at different temperatures

Table 3 Avrami exponents n and the correlation coefficients r^2 at different temperatures for samples BD-F3 and BD-F5

BD-F3			BD-F5		
Temperature T/°C	n	r^2	Temperature T/°C	n	r^2
856	5.56	0.9983	856	6.89	0.9983
858	5.14	0.9978	858	6.80	0.9985
860	5.49	0.9982	860	6.50	0.9995
862	5.41	0.9976	862	6.20	1.0
864	5.47	0.9965	864	6.71	0.9993
866	5.66	0.9950	866	6.69	0.9999
868	5.89	0.9933	868	6.91	0.9999
870	5.98	0.9934	870	6.75	0.9999
872	5.89	0.9950	872	6.54	1.0
874	5.73	0.9969	874	6.34	0.9997
876	5.55	0.9877	876	6.13	0.9988
878	5.36	0.9985			
880	4.63	0.9996			
882	4.56	0.9958			
884	4.52	0.9934			
886	5.29	0.9905			
888	5.39	0.9949			
890	5.37	0.9986			
892	5.30	1.0			
894	5.20	0.9982			
896	5.07	0.9931			

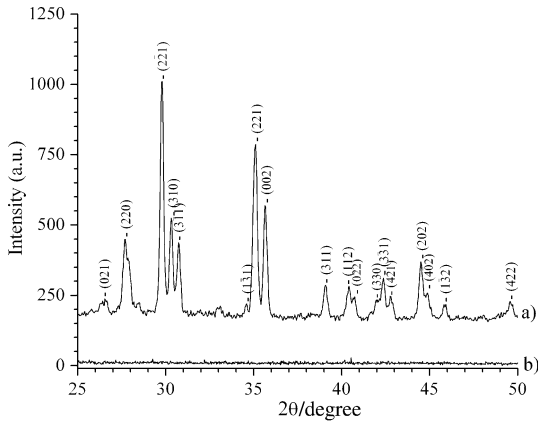

Fig. 9 X-ray diffraction patterns of sample BD-F3: **a** after thermal treatment at 900 °C, for 1 h; **b** before thermal treatment

The nature of the crystalline phase formed during the studied crystallization processes has been established by X-ray diffraction analysis. In Fig. 9 the X-ray patterns for the sample BD-F3 before and after thermal treatment at 900 °C, for 1 h are presented.

The results of the X-ray diffraction analysis reveals the presence of the pyroxene solid solution (JCPDS files 41-1370 and 41-1372) in the sample thermally treated at 900 °C, for 1 h.

Conclusions

The activation energies of the studied glass-ceramics (samples BD-F3 and BD-F5) calculated with four isoconversional methods show high values, of the order of hundreds kJ mol^{-1}. The activation energies calculated with KAS, Starink and Tang equations are very close and a little below the values obtained with the OFW method.

The increase of the nucleation agent content from 3% CaF_2 in the sample BD-F3 to 5% CaF_2 in the BD-F5 sample resulted in a decrease of the E_a values, regardless which isoconversional method was used.

The isoconversional analysis applied to the non-isothermal crystallization of the studied glass-ceramics shows the dependence of the activation energy on the crystallized fraction, which confirms that the crystallization mechanism is complex and the calculated activation energies are apparent values, depending on the activation energies of nucleation and crystallites growth.

The Avrami exponent calculated with Ozawa method has high values ($n > 4$) for both samples, indicating that the JMA model cannot be used for the crystallization of the studied glass-ceramics.

References

1. Pavluşkin NM. Osnovî tehnologii sitalo. Moskva: Stroizdat; 1977.
2. Kovacs G, PhD Thesis, Univ. Politehnica, Timişoara, 1997.
3. Torres FJ, Alarcon J. Pyroxene-based glass-ceramics as glazes for floor tiles. J Eur Ceram Soc. 2005;25:349–55.
4. Rincon JMa, Caceres J, Gonzalez-Oliver CJ, Russo DO, Petkova A, Hristov H. Thermal and sintering behaviour of basalt glasses and natural basalt powders. J Therm Anal Calorim. 1999;56:931–8.
5. Karamanov A, Ergul S, Akyildiz M, Pelino M. Sinter-crystallization of a glass obtained from basaltic tuffs. J Non-Cryst Solids. 2008;354:290–5.
6. Goel A, Shaaban ER, Melo FCL, Ribeiro MJ, Ferreira JMF. Non-isothermal crystallization kinetic studies on $MgO–Al_2O_3–SiO_2–TiO_2$ glass. J Non-Cryst Solids. 2007;353:2383–91.
7. Kovacs G, Lazău I, Menessy I, Kovacs K. Glass-ceramics from modified Şanoviţa(Timiş) basalt. Key Eng Mater. 1997;132–136:2135–8.
8. Junina LA, Kuzmenkov MI, Iaglov VN. "Piroxenovîie sitallî", Izd. B. G. U. Lenina, Minsk, 1974.
9. Samia NS, Saad MS, Hussein D. The effect of nucleation catalysts on crystallization characteristics of aluminosilicate glasses. Ceramics-Silikáty. 2002;46(1):15–23.
10. Păcurariu C, Liţă M, Lazău I, Tiţa D, Kovacs G. Kinetic study of the crystallization processes of some glass ceramics based on Basalt, via thermal analysis. J Thermal Anal Calorim. 2003;72:811–21.
11. Păcurariu C, Tiţa D, Lazău RI, Kovacs G, Lazău I. Kinetics of crystallization processes in some glass ceramic products. Influence of nucleation agents. J Therm Anal Calorim. 2003;72:823–30.
12. Khawam A, Flanagan DR. Role of isoconversional methods in varying activation energies of solid-state kinetics. II. Nonisothermal kinetic studies. Thermochim Acta. 2005;436:101–12.
13. Starink MJ. A new method for the derivation of activation energies from experiments performed at constant heating rate. Thermochim Acta. 1996;288:97–104.
14. Starink MJ. The determination of activation energy from linear heating rate experiments: a comparison of the accuracy of isoconversion methods. Thermochim Acta. 2003;404:163–76.
15. Sbirrazzuoli N, Vincent L, Bouillard J, Elegant L. Isothermal and non-isothermal kinetics when mechanistic information available. J Therm Anal Calorim. 1999;56:783–92.
16. Cai JM, Liu RH. Precision of integral methods for the determination of the kinetic parameters. Use in the kinetic analysis of solid-state reactions. J Therm Anal Calorim. 2008;91(1):275–8.
17. Starink MJ. Activation energy determination for linear heating experiments:deviations due to neglecting the low temperature end of the temperature integral. J Mater Sci. 2007;42:483–9.
18. Ozawa T. Kinetic analysis of derivative curves in thermal analysis. J Therm Anal. 1970;2(3):301–24.
19. Ozawa T. Kinetics of non-isothermal crystallization. Polymer. 1971;12:150–8.
20. Simon P. Isoconversional methods. Fundamentals, meaning and application. J Therm Anal Calorim. 2004;76:123–32.
21. Ozawa T. Kinetics of growth from pre-existing surface nuclei. J Therm Anal Calorim. 2005;82:687–90.
22. Chen HX, Liu NA. Approximations for the temperature integral. Their underlying relationship. J Therm Anal Calorim. 2008;92(2):573–8.
23. Doyle CD. Series approximations to the equations of thermogravimetric data. Nature. 1965;207:290–1.
24. Coats AW, Redfern JP. Kinetic parameters from thermogravimetric data. Nature. 1964;201:68–9.
25. Doyle CD. Estimating isothermal life from thermogravimetric data. J Appl Polym Sci. 1962;6:639–42.

26. Wanjun T, Yuwen L, Hen Z, Cunxin W. New approximate formula for Arrhenius temperature integral. Thermochim Acta. 2003;408:39–43.
27. Wanjun T, Donghua C. An integral method to determine variation in activation energy with extent of conversion. Thermochim Acta. 2005;433:72–6.
28. Avrami M. Granulation, phase change, and microstructure kinetics of phase change. J Chem Phys. 1941;9:177–85.
29. Malek J. Crystallyzation kinetics by thermal analysis. J Therm Anal Calorim. 1999;56:763–9.
30. Păcurariu C, Lazău RI, Lazău I, Tiţa D. Kinetics of non-isothermal crystallization of some glass-ceramics based on basalt. J Therm Anal Calorim. 2007;88(3):647–52.
31. Vlase T, Păcurariu C, Lazău RI, Lazău I. Kinetic studies of the crystallization process of one glass-ceramic based on basalt. J Therm Anal Calorim. 2007;88(3):625–9.